DOI: 10.15669/pnst.7.110

Progress in Nuclear Science and Technology
Volume 7 (2025) pp. 110-116

ARTICLE

Development of passive neutron emission tomography robust to its various inhibiting factors and its applicability to nuclear safeguards

Katsuyoshi Tsuchiya, Hiroshi Sagara * and Chi Young Han

Tokyo Institute of Technology, 2-12-1 Ookayama, Meguro-ku, Tokyo, 152-8550 Japan

The development of more sensitive and less intrusive non-destructive assay (NDA) instruments is one of the most urgent requirements in the long-term R&D plan of nuclear safeguards of the International Atomic Energy Agency (IAEA) for partial defect verification of spent fuel assemblies prior to their transfer to storage facilities that are difficult to access. As a promoting NDA technology, passive gamma emission tomography (PGET) has been developed to detect missing single fuel pins or the replacement with a dummy in the spent fuel assembly of a light water reactor. However, in PGET, image blurring occurs at the center of the fuel assembly because of the high self-attenuation of gamma in the fuel pins. Hence, passive neutron emission tomography (PNET) was initiated as an alternative to NDA technology, utilizing the fast neutrons easily exiting from inner spent fuel. However, in underwater measurements, neutron scattering and moderation by water hinder the acquisition of clear image. The objectives of this study are to validate the feasibility of PNET and verify its applicability to nuclear safeguards as an NDA technology for partial defect verification. PNET utilizes passive neutron measurements to obtain the projection profile of the intensity distribution of neutron sources at different detection angles. Numerical calculation were performed to validate the feasibility of PNET using a boiling water reactor (BWR) spent fuel assembly model and ideal black neutron absorber slits to discriminate the neutrons coming into the collimator. The neutron source information was calculated using SCALE6.2, and neutron transport to the detectors was calculated using MCNP6.2. The projection profile composed of the neutrons counts at each counting zone was reconstructed using maximum likelihood-expectation maximization (ML–EM) algorithm. The reconstructed images were examined based on the original fuel rod positions under in-air and underwater measurement conditions. The result showed that the reconstructed images obtained in the in-air measurements match the original ones, although intensive noise appears in the reconstructed images and the fuel rod positions were not identified in the underwater measurements. Detecting neutrons above 1 MeV is an effective technical solution for utilizing PNET underwater. Additionally, in terms of fuel rod dentification, the displacement by the scanning position and rotation angle errors should be less than the collimator slit width. The applicability of PNET as an NDA technology for nuclear safeguards was evaluated in terms of partial defect verification. Discriminant analysis was performed to statistically identify the replacement of fuel rods by dummy rods using relative values obtained by normalizing learning data. Using the discriminant conditions to identify defects with 97.5% reliability, the probability of defect detection and fuel rod false detection were evaluated to be 100% and 2% or less, respectively with several unknown partial defect models.

Keywords: passive neutron emission tomography; non-destructive assay; safeguards; spent fuel assembly

Nomenclature

NDA	Non-Destructive Assay	PWR	Pressurized Water Reactor
IAEA	International Atomic Energy Agency	BWR	Boiling Water Reactor
PGET	Passive Gamma Emission Tomography	ML-EM	Maximum Likelihood-Expectation Maximization
PNET	Passive Neutron Emission Tomography	ROI	Region of Interest

1. Introduction

The development of more sensitive and less intrusive non-destructive assay (NDA) instruments is one of the most urgent requirements in the long-term R&D plan of nuclear safeguards of the International Atomic Energy Agency (IAEA) for the partial defect verification of spent fuel assemblies prior to their transfer to storage facilities that are difficult to access [1]. As a promising NDA technology, passive gamma emission tomography (PGET), which utilizes passive gamma measurements to obtain the

*Corresponding author. E-mail: sagara.h.aa@m.titech.ac.jp

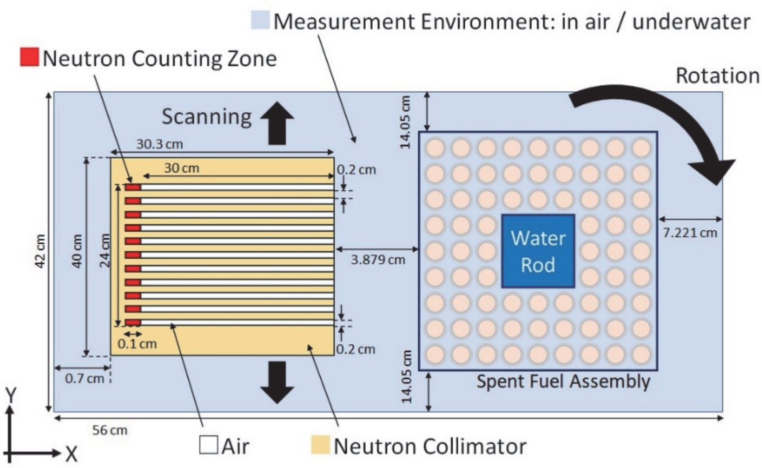

Figure 1. Calculation model.

projection profile of the intensity distribution of gamma sources at different detection angles, has been developed to detect missing single fuel pins or the replacement with a dummy in the spent fuel assembly of a light water reactor [2-5]. However, in PGET, image blurring occurs at the center of the fuel assembly because of the high self-attenuation of gamma in the fuel pins. Thus, research of detecting fast neutron from natural decay of spent fuel in a dry storage cask to obtain the neutron intensity of the spent fuel assembly was executed [6]. This research detects neutrons from top side of the cask and only creates two-dimensional intensity distribution. The results were superior to the Fingerprinting method [7] but limited only two-dimension since the leakage from the side of the cask is limited and the neutron emitted from the outside of the cask actively is also limited. Hence, to obtain the three-dimensional intensity distribution, passive neutron emission tomography (PNET) was initiated as an alternative to NDA technology [8-10]. Fast neutrons exiting spent fuel will penetrate the inner fuel pins with a high probability. Measurement of neutron sources in air is expected to provide a clear projection profile. In fact, the previous study clarified the measurement conditions and specifications satisfying the requirement for partial defect verification of a pressurized water reactor (PWR) spent fuel assembly in the air. However, in underwater measurements, neutron scattering and moderation by water will hinder the acquisition of a clear projection profile. This water impact has not been evaluated and the number of previous research of PNET is limited. In addition, the maximum likelihood–expectation maximization (ML–EM) was adopted in the tomograph technology field but was not applied to the neutron counting. The objectives of this study are to validate the feasibility of PNET and verify its applicability to nuclear safeguards as an NDA technology for partial defect verification.

2. Methodology and validation of PNET

A numerical calculation model was created to validate the feasibility of PNET, as shown in **Figure 1**. A boiling water reactor (BWR) spent fuel assembly (9 × 9, step 3, type B, 39.92 GWd/t, no cooling [11] was modeled to obtain the projection profile of the neutron sources, as shown in **Figure 2.** The neutrons incoming into the collimator were discriminated by slits (measuring 0.2 cm wide and 30 cm long) that were split at every 0.2 cm-wide ideal black neutron absorber. Sixty neutron-counting zones occupying a width of 24 cm were set in the calculation model. The neutron source information emitted from the BWR spent fuel assembly was calculated using SCALE6.2, and neutron transport to the counting zones was simulated using MCNP6.2. To eliminate the effect of neutron leakage in the z-direction, which is parallel to the assembly, the height of the assembly was set sufficiently high, and the direction of neutron emission was fixed perpendicular to the fuel rods. From this assumption, the leakage of z-direction could be ignored. Tomography to obtain the projection profile of the neutron intensity distribution was performed by rotating the spent fuel assembly 360°, where every 1° of neutron scanning (detection) in the collimator was conducted at both its original position and 0.2 cm shift in the y-direction. Subsequently, 120 sets of projection data were obtained at each angle. The projection profile was reconstructed into a two-dimensional cross-sectional image using the ML–EM

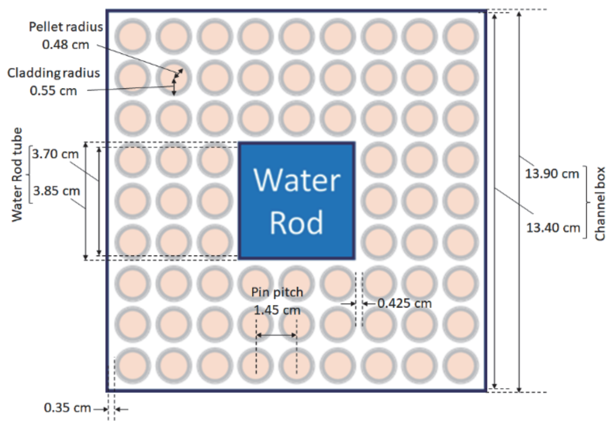

Figure 2. Specifications of BWR spent fuel assembly [13].

algorithm [12]. Neutron measurements were performed under both air and underwater conditions to confirm the effect of water on PNET.

Figure 3 shows the reconstructed images for neutron counts per source neutron in the air and underwater measurement conditions. The reconstructed image in the air measurement condition clearly shows the original fuel rods; however, an intensive noise appeared in the underwater measurement and the fuel rods were not identified underwater. To reduce noise, a low-energy cut-off of neutrons in the MCNP simulation was examined to terminate the transport of scattered and moderated neutrons. The sensitivity of neutron cut-off energy to the reconstructed image was analyzed, and **Figure 4** shows the reconstructed images calculated using different neutron cut-off energy levels in the underwater measurement. The result indicates that filtering less than 1 MeV neutrons can effectively reduce noise by low-energy scattering neutrons and that utilizing high-energy sensitive neutron detectors allows PNET technology to be applied underwater. Subsequently, the effect of the collimator slits filled with water instead of air was examined. **Figure 5** shows a comparison of the reconstructed images in two cases involving the underwater measurement condition. The result shows that water in the slits significantly disperses the image by more scattering and capture of neutrons. Filling the collimator slits with air is necessary to apply the PNET technology underwater. In case of practical implementation, partition panels are necessary to divide water areas and air areas. The material condition should be small capture and scattering cross-section and high strength against water pressure since deep location of spent fuel assembly in a cooling pool. The exploration of suitable materials is another research topic.

The sensitivity to mechanical errors in measurement, such as scanning position error and rotation angle error, was investigated. The scanning position error was assumed to exhibit three different displacements, i.e., ±0.1 cm, ±0.2 cm, and ±0.3 cm, in the y-direction of the original scanning. For each case, the projection data were averaged at three positions: no displacement (original position),

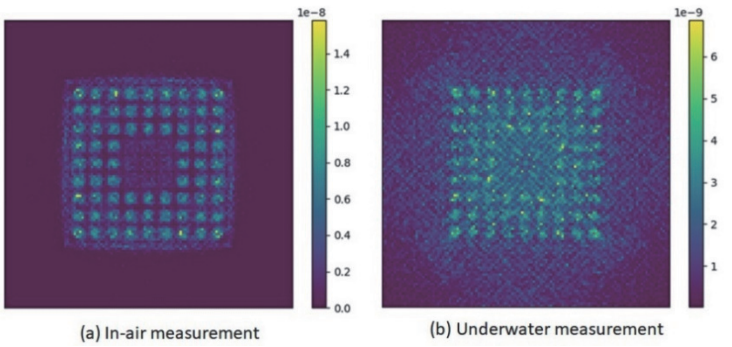

Figure 3. Reconstructed images with measurement condition.

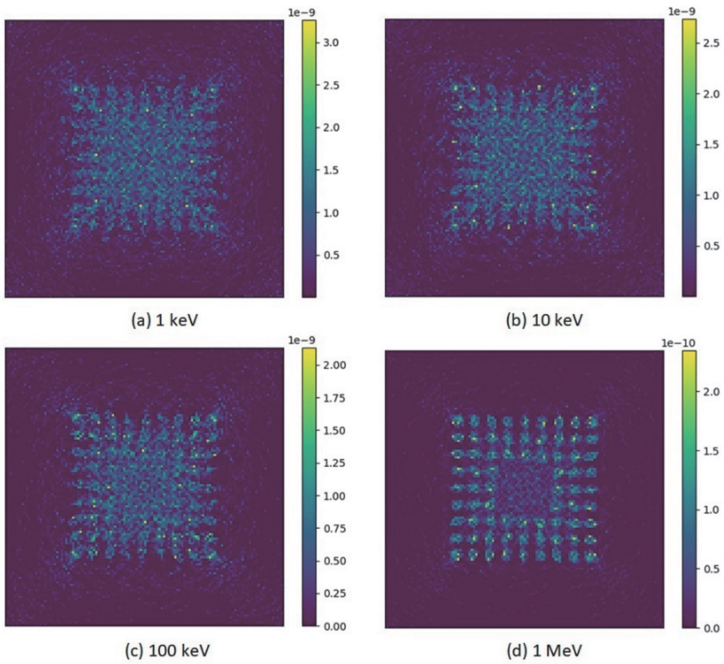

Figure 4. Reconstructed images with neutron cut-off energy in underwater measurement condition.

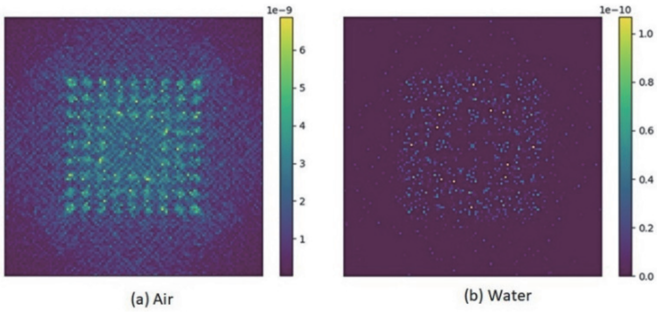

Figure 5. Reconstructed images with collimator slit material in underwater measurement condition.

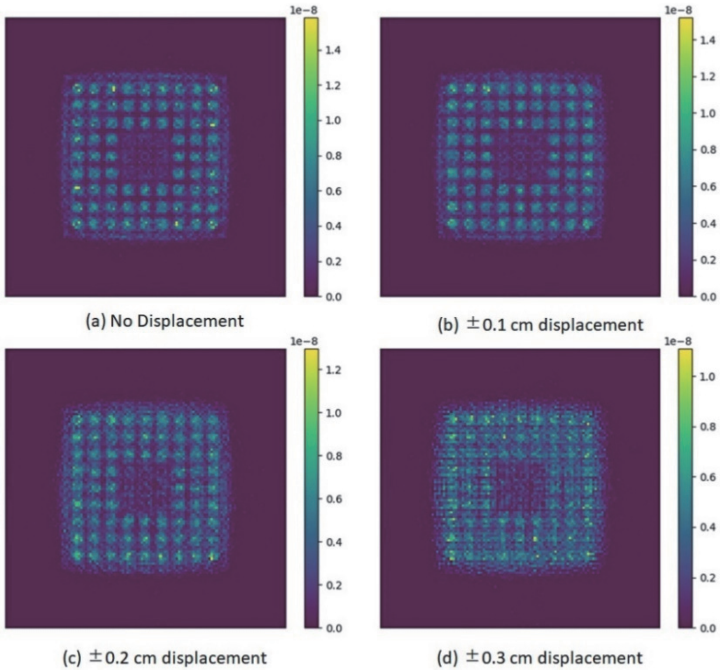

Figure 6. Reconstructed images with scanning position error in air measurement condition.

plus displacement, and minus displacement in the direction. **Figure 6** shows the reconstructed images calculated using the scanning position errors under the air measurement conditions. A scanning position displacement exceeding 0.2 cm corresponding to the collimator slit width reduces the resolution of the reconstructed images. The slit width should be less than the radius of the fuel rod to identify it and the scanning position error should be smaller than the slit width to acquire a clearer image. The projection data were averaged at three positions, i.e., no displacement (original position), plus displacement, and minus displacement in the rotation direction. **Figure 7** shows the reconstructed images calculated using the rotation angle errors. An angular displacement exceeding ±2° reduces the resolution of the reconstructed images, particularly in the corner of the fuel assembly. For the outermost fuel pin in the corner, an angular displacement of 2° was observed when the position displacement exceeded 0.2 cm in the rotation direction. The results of the sensitivity analysis indicate that the displacement by the scanning position and rotation angle errors should be less than the collimator slit width (the pixel size of the reconstructed image).

3. Applicability of PNET to nuclear safeguards

The applicability of PNET as an NDA technology for nuclear safeguards was evaluated for partial defect verification. Discriminant analysis was performed to statistically identify the replacement of fuel rods by dummy rods. The dummy rods were assumed as stainless-steel rods. Twelve sets of partial defect models were constructed, and their reconstructed images were obtained as learning data for in-air and underwater measurements, respectively. The region of interest (ROI) was set at 72 fuel rod positions in the reconstructed images, and the intensity inside the ROI was obtained at the fuel rod and dummy rod positions. All detected neutron intensities were graded from a maximum of 255 to a minimum of 0, as well as by the intensity of the fuel and dummy rods. Assuming a normal distribution of the intensity, the detected neutron intensities in the fuel and dummy rods were discriminated at the line on the right side of 2σ of the dummy rod normal distribution to identify defects with 97.5% reliability. The discriminant conditions of the in-air and underwater measurements were validated via hypothesis

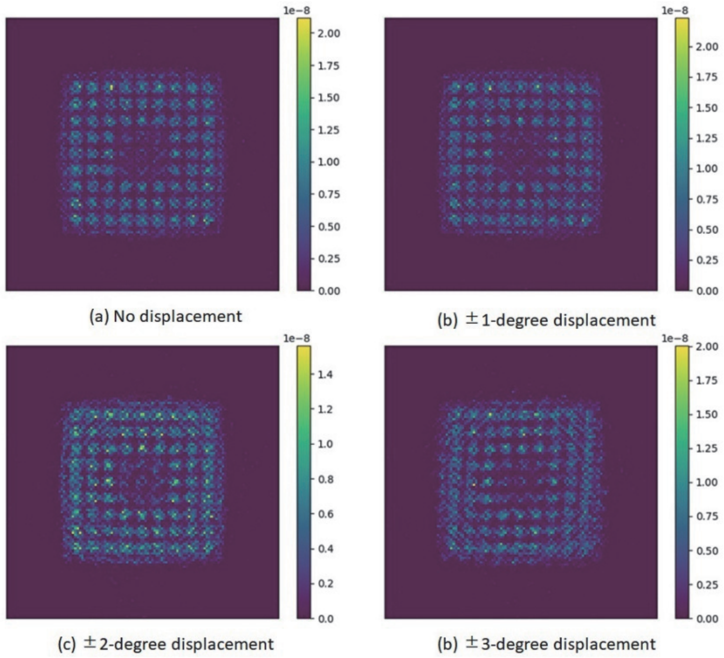

Figure 7. Reconstructed images with rotation angle error in air measurement condition.

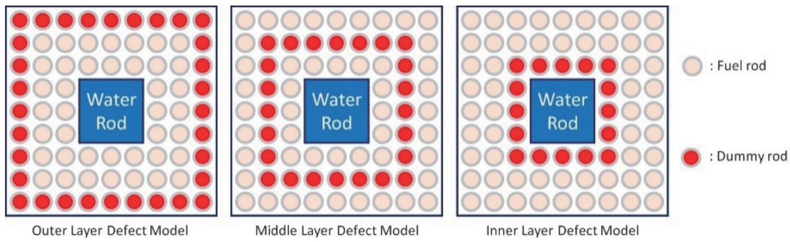

Figure 8. Partial defect models.

testing. The null hypothesis is that the obtained intensities greater than the discriminant condition value are from the fuel rods, and the alternative hypothesis is that the obtained intensities under the discriminant condition value are from defects. Setting the level of significance at 5%, the integral value of the fuel rods originating from $-\infty$ to t, which is the discriminant condition value, was calculated for the type I error of which value corresponds to the probability of mis-identifying the partial defects as fuel rods. The process was applied to in-air and underwater measurement conditions; consequently, the type I error values for the in-air and underwater conditions were 7.34×10^{-6} and 3.64×10^{-3}, respectively. Therefore, the mis-identification probability was lower than the level of significance, and thus the null hypothesis was rejected.

These discriminant conditions were applied to several unknown partial-defect models. The outer layer defect model (defects of outer layer fuel rods), middle layer defect model (defects of middle layer fuel rods), and inner layer defect model (defects of inner layer fuel rods) were prepared as partial defect models and shown in **Figure 8**. Reconstructed images under in-air and underwater measurement conditions of each model were obtained, and the neutron intensities inside the ROI were normalized as described above. The discrimination conditions were applied to the normalized intensities, and the numbers of fuel and dummy rods were estimated. The actual values of the fuel and dummy rods were known; hence, the difference between the actual and estimated values was calculated. The probabilities of defect detection and fuel rod false detection were calculated by dividing each difference by the actual value.

The verification results of the discriminant conditions applied to several partial-defect models are shown in **Figure 9**. The horizontal axis in each histogram represents the detected neutron intensities which is from 0 to 255 as mentioned. The vertical axis in each histogram represents the number of fuel and dummy rods corresponding to every detected neutron intensity, and the summation of the vertical axis value at every intensity must be 72 that is the number of fuel rods and dummy rods. In the outer and middle layer defect models, the estimated values obtained with the discriminant conditions agreed well with the actual values under in-air and underwater measurement conditions. Meanwhile, in the inner layer defect model, the estimated value in the in-air measurement condition matched the actual value, although one fuel rod was erroneously discriminated as a dummy rod in the underwater measurement condition. Based on the results, the probability of defect detection was evaluated to be 100%, and the probability of false fuel

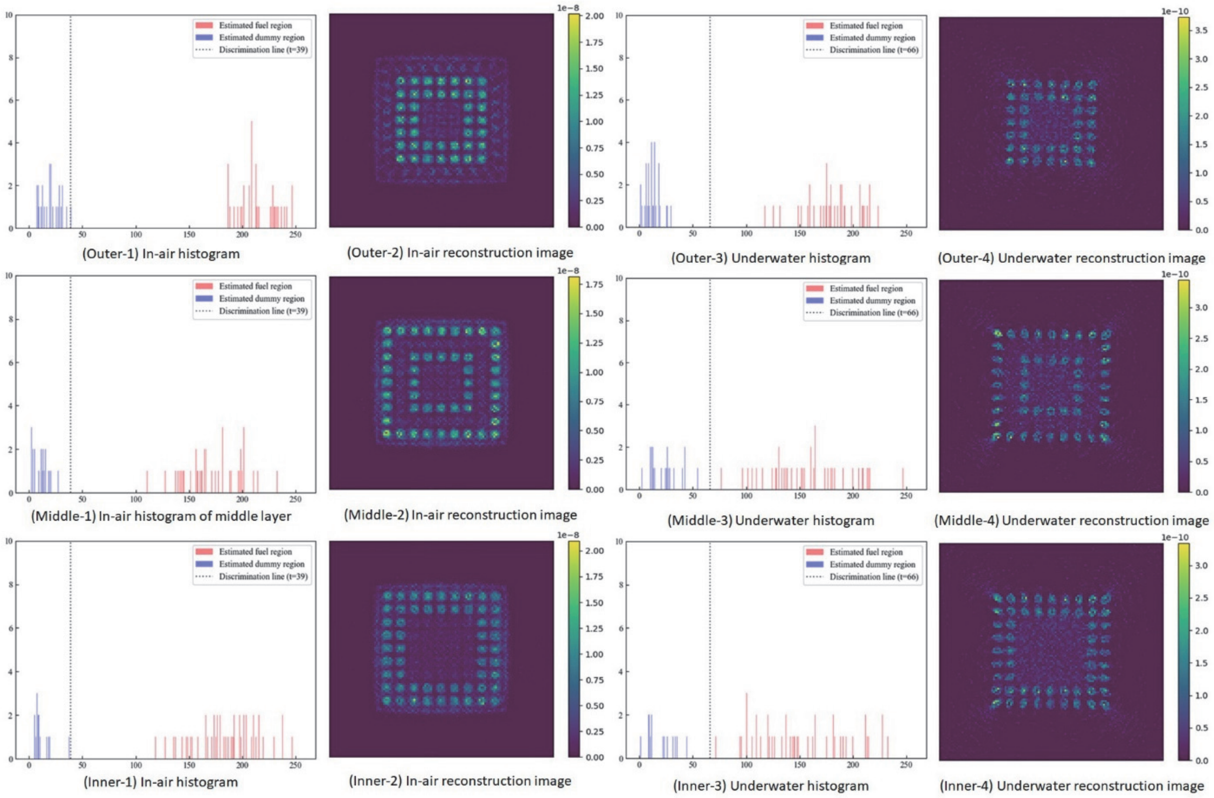

Figure 9. Histogram and reconstructed image of defect of inner layer pins.

rod detection was 2% or less. This performance satisfied the IAEA safeguards requirement for partial defect verification that is detection of 50% removal or substitution of nuclear material from the inspected item [14,15], and the discriminant conditions were shown to be valid.

4. Conclusion

The principle of PNET was validated and its applicability to nuclear safeguards as an NDA technology for partial defect verification was verified numerically. Reconstructed images obtained under in-air measurement conditions were consistent with the original fuel rod position. However, intensive noise caused by scattered and moderated neutrons appeared in the reconstructed image, and the fuel rod positions were not identified under underwater measurement conditions. Detecting neutrons above 1 MeV would be an effective technical solution for utilizing PNET in underwater measurement conditions to eliminate noise. In addition, in terms of fuel rod identification, the displacement by the scanning position and rotation angle errors should be less than the collimator slit width. The applicability of PNET as an NDA technology for nuclear safeguards was evaluated in terms of partial defect verification. Discriminant analysis was performed using relative values obtained by normalizing learning data. Using the discriminant conditions to identify defects with 97.5% reliability, the probability of defect detection and fuel rod false detection were evaluated to be 100% and 2% or less, respectively.

References

[1] International Atomic Energy Agency, IAEA Department of Safeguards Long-Term R&D Plan, (2019), 2012–2023, (STR-375). International Atomic Energy Agency, Vienna.

[2] S. Shiba and H. Sagara, MLEM reconstruction method applied to partial defect verification using simulated data, *Ann. Nucl. Energy*. 139 (2020a), 107242.

[3] S. Shiba and H. Sagara, Fast reconstruction of Bayesian iterative approximation in passive gamma-ray tomography, *J. Nucl. Sci. Technol*. 57 (2020b), pp. 546-552.

[4] S. Shiba and H. Sagara, Passive gamma emission tomography with ordered subset expectation maximization method, *Ann. Nucl. Energy*. 150 (2021a), 107823.

[5] S. Shiba and H. Sagara, Iterative reconstruction algorithm comparison using Poisson noise distributed sinogram data in passive gamma emission tomography, *J. Nucl. Sci. Technol*. 58 (2021b), pp. 659-666.

[6] Y. Ham, S. Sitaraman and P. Kerr, Verification of Spent Fuel Inside Dry Storage Casks Using Fast Neutrons, *LLNL-CONF-773319* (2019).

[7] K.P. Ziock, P. Vanier, L. Forman, G. Caffrey, J. Wharton and A. Lebrun, The Feasibility of Cask “Fingerprinting” as a Spent-Fuel, Dry-Storage Cask Safeguards Technique, CURL-TR-215943, (2005).

[8] T. Tokuda, S. Shiba and H. Sagara, Development of Non-Destructive Assay Technique using Passive Neutron Emission Tomography and Applicability for

Partial Defect Verification, in: *Proc. 41st INMMJ Ann. Mtg*. (2020).

[9] K. Tsuchiya, , H. Sagara and C.Y. Han, Non-estructive Assay Technology Using Passive Neutron Emission Tomography -Inhibiting Factor Sensitivity of Tomography Image-, in: *Proc. 42nd INMMJ Ann. Mtg*. (2021).

[10] K. Tsuchiya, T. Tokuda, H. Sagara and C.Y. Han, Development of Passive Neutron Emission Tomography and Its Applicability to Nuclear Safeguards, in: *Proc. 63rd INMM Ann. Mtg*. (2022).

[11] Y. Nakahara, K. Suyama, and T. Suzaki, Technical development on burn-up credit for spent LWR fuels, *Jpn At. Energy Res. Inst. JAERI-Tech*. (2000), 071.

[12] K. Sakaguchi, H. Shinohara and T. Hashimoto, Implementation of maximum-likelihood-expectation maximization method in Excel. *J. Jpn Acad. Health Sci*. (2006) pp. 264-280.

[13] OECD. NEA, Burn-up Credit Criticality Safety Benchmark Phase III-C, March, 2016.

[14] International Atomic Energy Agency, IAEA Safeguards Glossary In International Nuclear Verification Series, Vol. 3, 2001 ed.

[15] B. Erik, Enhancing the performance of the Digital Cherenkov Viewing Device: Detecting partial defects in irradiated nuclear fuel assemblies using Cherenkov light, (2018).